ELSEVIER

Journal of Chromatography A, 773 (1997) 13–22

JOURNAL OF CHROMATOGRAPHY A

Modelling gradient elution in centrifugal partition chromatography

Michel J. van Buel, Luuk A.M. van der Wielen*, Karel Ch.A.M. Luyben

Department of Biochemical Engineering, Delft University of Technology, Julianalaan 67, 2628 BC Delft, The Netherlands

Received 2 December 1996; revised 17 February 1997; accepted 26 February 1997

Abstract

Varying the phase composition of a multi-component two-phase system during a centrifugal partition chromatography (CPC) separation leads to additional degrees of freedom to influence the separation efficiency and total separation time. Optimisation of a CPC (gradient) separation is a difficult task due to the large number of two-phase systems and the different elution modes that can be applied. A model is presented that predicts effluent concentration profiles of gradient elution, given the partition coefficients of the components and a mass transfer relationship as a function of the local phase composition, at a fixed flow-rate, stationary phase hold-up and rotational frequency. The model is verified by comparing the results of simulated effluent concentration profiles to experimental effluent concentration profiles. It is shown how the composition-dependent parameters needed for the model predictions can be accessed experimentally. By performing model aided optimisation of CPC separations the time needed for optimising a gradient elution, and the need for laborious experimental work is reduced significantly. © 1997 Elsevier Science B.V.

Keywords: Counter-current chromatography; Centrifugal partition chromatography; Gradient elution; Mathematical modelling; Phenols

1. Introduction

Centrifugal partition chromatography (CPC) is a novel chromatographic technique in which the separation mechanism is based on different migration velocities of components due to their difference in partitioning over two immiscible liquid phases. A CPC column consists of stacked polymer plates, which are placed in a centrifuge. In the polymer plates, channels are engraved that are connected by narrow ducts. The stationary phase stays in the channels due to the centrifugal force and the special column geometry. The mobile phase flows through the stationary phase in the form of droplets, jets or breaking jets depending on the operating conditions [1]. If the dense phase is used as the mobile phase, the mobile phase should enter the channel at the side of the rotor axis. Due to the centrifugal force, the stationary phase is pushed in the direction of the rotor axis while the mobile phase moves away from the rotor axis. This is called the descending mode. If the light phase is used as the mobile phase, the mobile phase should enter the channel at the other side (compared to the descending mode). This is called the ascending mode. Commercially available columns can consist of 800 or more channel–duct combinations. The total volume of a CPC column can range from 40 ml for a semi-analytical column to 30 l for a preparative column. Different cartridge and channel geometries are possible [2,3]. Any binary or multicomponent mixture of liquids, giving a two-phase system can be applied. This enables fine-

*Corresponding author.

PII S0021-9673(97)00245-8

tuning of the separation system for a specific mixture of components to be separated. An overview of separations that have been performed by CPC are given by Foucault [4] and Marston and Hostettmann [5]. An extensive list of the more general literature presented on the subject of CPC is given by Conway [6].

An elution mode suitable to perform separations, with components with large differences in partition coefficients, is the gradient elution mode. During a separation with the gradient elution mode the composition of the mobile phase is changed, while the composition of the stationary phase is kept (almost) constant. Examples of separations using the gradient elution mode are the separation of amino acids and peptides with hexane–1-butanol–water two-phase systems [7], chromomycins with the toluene–2-butanone–methanol–water two-phase system [8] and flavonols from a commercialised extract of *Grinkgo biloba* leaves with the ethyl acetate–2-butanol–water system [9]. Not all ternary two-phase systems are suitable for gradient elution. To prevent instability of the stationary phase during a gradient run the change in stationary phase composition should be small (<20% v/v). Foucault and Nakanishi [7] have shown that the two-phase system hexane–methanol–water, is very suitable for gradient elution. No loss in stationary phase was observed during gradient elution. The reason is that when the composition (predominantly water–methanol) of the mobile phase is changed, the composition of the stationary phase (predominantly hexane) hardly changes. Foucault and Nakanishi [10] gave an overview of two-phase systems that are suitable for gradient elution. A system that shows great potential for the separation of a wide variety of components from a natural source is chloroform–methanol–water [7].

Optimisation of the gradient with respect to component purity and the total separation time is still very much based on 'trial and error'. The aim of this work, is to present a model that describes effluent concentration profiles of gradient elution experiments. The model is verified by comparing simulated effluent concentration profiles with experimental effluent concentration profiles. The two-phase system used for the gradient elution experiments is heptane–methanol–water (HMW) with chloromethylated phenols as model components.

2. Theory

2.1. Plug flow model

Van Buel et al. [11] derived a model describing CPC effluent concentration profiles assuming plug flow with axial dispersion of the mobile phase, while exchanging mass with a 'non-mixed' stationary phase. The concentration profile of a component eluting from the column is described as a function of its partition coefficient (K), its overall volumetric mass transfer coefficient ($k_o a$) and a Péclet number (Pe) as a measure for mobile phase mixing. The three parameters are obtained by comparing experimental concentration profiles with model predictions. Peak broadening due to mixing outside the column (tubing, rotary seals, pressure transmitter) is corrected for by using effluent concentration profiles measured without the column present in the experimental setup.

The Péclet number is obtained from effluent concentration profiles of a component that does not partition to the stationary phase and therefore elutes from the column unretained. The additional peak broadening (additional to mixing outside the column) of this component is consequently caused by mixing in the mobile phase in the column only. Van Buel et al. [11] showed that the Péclet number was large (>2000) and independent of the experimental conditions, which means that the influence of mixing on peak broadening is relatively small.

The overall volumetric mass transfer coefficient and the partition coefficient of a component that partitions to the stationary phase are also obtained by comparing experimental effluent concentration profiles to model predictions. Van Buel et al. [11] showed that the fitted partition coefficients compare well with partition coefficients obtained from shake flask experiments. The overall volumetric mass transfer coefficient ($k_o a$) is the product of the overall mass transfer coefficient (k_o) and the specific interfacial area (a).

The resulting set of mass balances for a component i is:

$$\frac{\partial X_i}{\partial \Theta} + \frac{\partial X_i}{\partial z} - \frac{1}{Pe}\frac{\partial^2 X_i}{\partial z^2} = -StK_i(X_i - Y_i) \qquad (1)$$

$$\frac{\partial Y_i}{\partial \Theta} = \frac{(1-\varepsilon_s)}{\varepsilon_s} St(X_i - Y_i) \quad (2)$$

where Θ is the dimensionless time, t/τ, with τ the residence time of the mobile phase, ε_s is the stationary-phase hold-up (stationary phase volume divided by the column volume), z is the dimensionless position in the column, X and Y are the dimensionless mobile and stationary phase concentrations, respectively, and St is the Stanton number defined as:

$$St = \frac{k_o a V}{\phi_v} \quad (3)$$

where V is the column volume and ϕ_v is the mobile phase flow-rate. The boundary conditions for the set of partial differential Eq. (1) and Eq. (2) are:

$$X_i(\Theta = 0, z) = 0 \quad (4)$$

$$Y_i(\Theta = 0, z) = 0 \quad (5)$$

$$X_i(\Theta, z = 0) = X_i^o(\Theta) \quad (6)$$

where X_i^o is an arbitrary input concentration profile.

2.2. Numerical solution

The set of partial differential Eqs. (1) and (2) is solved numerically by backward spatial discretisation using finite differences [12]. Neglecting axial dispersion, the set of partial differential equations thus becomes:

$$\frac{\partial X_i^n}{\partial \Theta} = -\frac{X_i^n - X_i^{n-1}}{\Delta z} - StK_i(X_i^n - Y_i^n) \quad (7)$$

$$\frac{\partial Y_i^n}{\partial \Theta} = \frac{1-\varepsilon_s}{\varepsilon_s} St(X_i^n - Y_i^n) \quad (8)$$

where n denotes the n^{th} discretisation step and $1/\Delta z$ equals the number of spatial discretisation steps. The set of differential equations was solved with a fourth order Runge Kutta algorithm. The parameters that are needed to perform the simulations are the mobile phase flow-rate, the stationary-phase hold-up, the column volume, and a partition coefficient and a mass transfer relationship for the given experimental conditions (both as a function of the gradient). For the simulations 300 stages were sufficient to prevent numerical dispersion. An experimental effluent concentration profile measured without the column present in the set-up, was used as the input signal (X_i°) for the simulations.

2.3. Partition coefficient as a function of the local composition

Experimental partition coefficient data, for 2-pentanone and 2-butanone as a function of the total volumetric water content (w) of the heptane–methanol–water two-phase system shows a linear relationship between ln K_i and w in the range 12.5–37.5% (v/v) [8]. Therefore, the partition coefficients of the chloromethylated phenols were fitted with the empirical relationship:

$$K_i = A_{i,1} e^{A_{i,2} w} \quad (9)$$

where $A_{i,1}$ and $A_{i,2}$ are constants for component i. It should be emphasised that the empirical relationship was used to facilitate numerical calculations and is only valid for this specific example. With other phase systems and/or components a more detailed thermodynamic description of the partitioning behaviour might be more appropriate, however, this was not the aim of this article.

2.4. Overall volumetric mass transfer coefficient as a function of the local composition

Van Buel et al. [11] have shown that the overall volumetric mass transfer coefficient depends on the partition coefficient according to:

$$\frac{1}{k_o a} = \frac{K_i}{k_m a} + \frac{1}{k_s a} \quad (10)$$

where $k_m a$ and $k_s a$ are the individual volumetric mass transfer coefficients in the mobile phase and stationary phase, respectively. The values for the individual volumetric mass transfer coefficients depend on the experimental conditions: flow-rate, rotational frequency, stationary-phase hold-up, the type of column and the two-phase system that is used. The latter is especially important since the composition of the two-phase system changes during a gradient elution separation.

The total water content of the two phase system at

stage n as a function of time Θ ($w_n(\Theta)$) was calculated from:

$$w_n(\Theta) = w_o\left(\Theta - \frac{nV_{stage}}{\phi_v \tau}\right) \quad (11)$$

where w_o is the total water content of the two-phase system at the inlet of the column as a function of time Θ (the actual gradient) and V_{stage} is the mobile phase volume for a stage. For calculation of the partition coefficients and the individual volumetric mass transfer coefficients as a function of the local composition, it was assumed that $w_n(\Theta)$ was independent of the stationary phase composition at a stage.

3. Materials and methods

3.1. The HPCPC column

Chromatographic experiments were performed with a HPCPC series 1000 centrifugal partition chromatograph purchased from Sanki Engineering. The column consists of 2 cartridges with 1068 channels each. Each cartridge has a volume of 103±3.0 ml. For the experiments one cartridge was used. More information on the HPCPC cartridge can be found in Foucault [2].

3.2. Materials

Methanol (HPLC grade) was purchased from Acros (Geel, Belgium), n-heptane (analytical-reagent grade) was purchased from Merck (Darmstadt, Germany) and 2-propanol (analytical-reagent grade) was purchased from J.T. Baker (Deventer, Netherlands). Water was demineralised. Three different two-phase systems were used for the experiments: heptane–methanol–water (50:37.5:12.5%, v/v) (HMW 12.5), heptane–methanol–water (50:25:25, v/v) (HMW 25) and heptane–methanol–water (50:12.5:37.5, v/v) (HMW 37.5). The solutes that were used are given in Table 1.

3.3. Determination of K as a function of the mobile phase composition with shake flask experiments

Shake flask experiments were performed to determine the partition coefficient by weighing the solute into the equilibrated two-phase system (±10 ml of each phase) by stirring it vigorously overnight in a water bath at 25°C. Directly after removal from the water bath the phases were separated and analysed by GC. The experiments were performed with Chrompack bottles of 50 ml with PTFE caps.

3.4. Gradient elution

The experimental set-up is shown in Fig. 1. An experiment was started by rinsing the column with all the tubing and the pressure drop meter with acetone (at 200 rpm in the ascending mode to remove air from the column) and filling the column with stationary phase (top phase of the HMW 37.5 system). Subsequently, the column was removed from the loop with a loop valve and the volume without the column was rinsed with acetone. Then one pump (Shimadzu LC-8A) was rinsed with the bottom phase of the HMW 37.5 system and the other identical pump with the bottom phase of the HMW 12.5 system. The tubing was rinsed with the bottom phase of the HMW 37.5 phase. The CPC was

Table 1
Supplier and purity of model components

Component	Supplier	Purity
Phenol	Fluka Biochemika	>99.5
2,4-Dimethylphenol	Fluka AG	≈90%, 5.7% 2,5 dimethylphenol
2,4-Dichloro-5-methylphenol	Aldrich	unknown
2,4-Dichloro-3,5-dimethylphenol	Aldrich	unknown

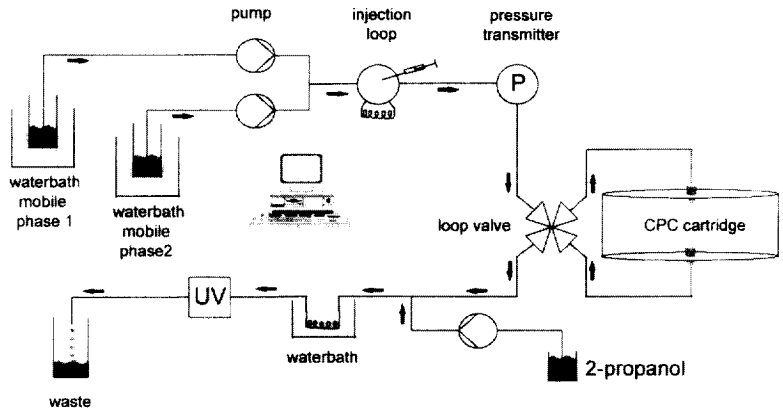

Fig. 1. Schematic drawing of the experimental set-up used for gradient elution.

switched to the descending mode and the rotational frequency was increased to 600 rpm. The loop valve was opened and the bottom phase of the HMW 37.5 system was pumped through the column at 6 ml/min. When the first mobile phase broke through, the rotational frequency was increased to 800 rpm and the flow-rate was decreased to 4 ml/min. The stationary-phase hold-up of the column was determined by collecting the stationary phase that flows from the column during filling with the mobile phase. All experiments were performed at 4 ml/min, 800 rpm. The mobile phase gradient was formed by varying the flow-rates of the two pumps. To obtain a stable baseline, 1 ml/min of 2-propanol was added after the mobile phase left the CPC, with a Waters 6000A pump. Components were injected with a Rheodyne 7125 injection valve equipped with a 200-μl injection loop. The components were dissolved in the mobile phase of the HMW 22.5 system, because the solubility of 2,4-dichloro-3,5-dimethylphenol (DCDMP) was not high enough in the HMW 37.5 system. The mobile phase was kept at a constant temperature of 25°C in a water bath.

4. Results

To be able to perform model simulations, values are needed for the partition coefficients and the individual volumetric mass transfer coefficients ($k_s a$ and $k_m a$) as a function of the local mobile phase composition.

4.1. Determination of the partition coefficient as a function of the mobile phase composition

The partition coefficients for w is 12.5% (v/v), 25% (v/v) and 37.5% (v/v), for phenol, 2,4-dimethylphenol (DMP), 2,4-dichloro-5-methylphenol (DCMP) and 2,4-dichloro-3,5-dimethylphenol are shown in Fig. 2. The error in the measured partition coefficient is roughly 5%. The constants $A_{i,1}$ and $A_{i,2}$ are given in Table 2 for phenol, DMP, DCMP and

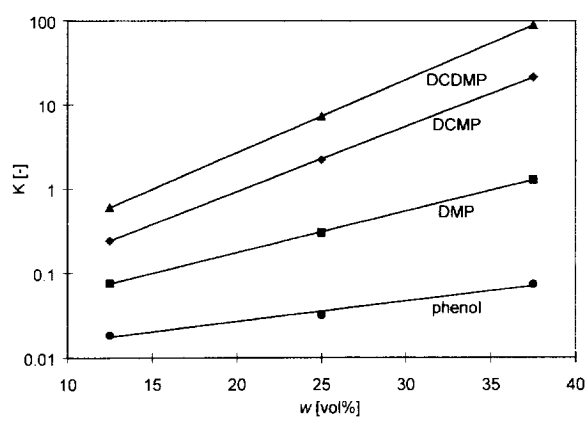

Fig. 2. K as a function of w. Markers are experimental data, lines are fitted with Eq. (9).

Table 2
Coefficient $A_{i,1}$ and $A_{i,2}$ for phenol, DMP, DCMP, DCDMP [Eq. (9)].

Component	$A_{i,1}\cdot 10^3$	$A_{i,2}\cdot 10^2$
Phenol	8.8±1.7	5.6±0.7
DMP	18±0.5	11±0.1
DCMP	26±1.1	18±0.1
DCDMP	49±0.6	20±0.1

Table 3
$1/k_s a$ and $1/k_m a$ for w is 12.5% (v/v), 25% (v/v) and 37.5% (v/v) [Eq. (10)]

w (%, v/v)	$1/k_s a$ (s)	$1/k_m a$ (s)
12.5	15.4±0.4	24.6±1.9
25	16.9±0.8	30.2±1.0
37.5	15.3±3.3	36.6±3.0

DCDMP. Fig. 2 clearly shows that Eq. (9) gives a good representation of the data for this specific case.

4.2. Determination of $1/k_s a$ and $1/k_m a$ as a function of the mobile phase composition

Fig. 3 shows $1/k_0 a$ as a function of K for w is 12.5% (v/v), 25% (v/v) and 37.5% (v/v). The experiments were performed at a flow-rate of 4 ml/min, a rotational frequency of 800 rpm and a stationary-phase hold-up of 0.75±0.01. Components with different partition coefficients were injected and the resulting concentration profiles were fitted with the model previously described by Van Buel et al. [11]. The experimental data were fitted with Eq. (10). The slope and the intercept with the y-axis are equal to $1/k_m a$ and $1/k_s a$, respectively, and are given in Table 3. The inverse individual volumetric mass transfer coefficients as a function of the local composition ($w_n(\Theta)$) were obtained by linear interpolation between the available points for w is 12.5% (v/v), 25% (v/v) and 37.5% (v/v).

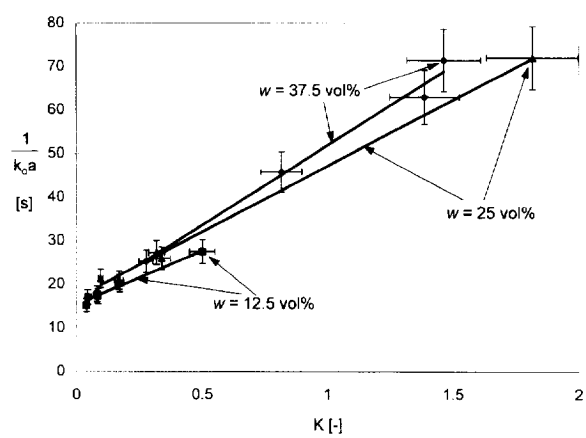

Fig. 3. Inverse overall volumetric mass transfer coefficient as a function of the partition coefficient. Markers are experimental data, lines are fitted with Eq. (10).

4.3. Comparison between model predictions and experiments

To demonstrate the predictive capabilities of the model, experiments with different gradients were performed. The injected components, the stationary-phase hold-up and the gradients for the different experiments are given in Table 4. Fig. 4 shows the experimental and simulated results for gradient 1. The individual simulated effluent concentration profiles have been normalised with respect to the experimental effluent concentration profiles. The simulated effluent concentration profiles of DCMP and DCDMP have been combined after normalisation. Unfortunately, a slight variation in the baseline of the experimental effluent concentration profile could not be prevented. The experiment with gradient 1 was repeated five times to determine the variation in the experimental retention times and the experimental peak widths of DMP, DCMP, DCDMP (phenol elutes before the gradient starts). The average experimental retention time and the retention time of the simulated peaks are given in Table 5. The error in the average experimental retention time is based on the maximum deviation from the average value. The error is approximately equal to the estimated error in the stationary-phase hold-up. This indicates very reproducible gradient experiments. Although, the prediction of the retention time is good, it appears from Fig. 4 as if the model predicts retention times that are too small. This might be due to the error in the column volume (±3%) or the error in the measured partition coefficients (±5%). The average peak widths of the experimental and the simulated peaks are also presented in Table 5. The error in the experimental peak width is based on the

Table 4
Experimental conditions

Gradient number	Stationary-phase hold-up	Gradient		Components + concentration (g/l) in HMW 22.5
		Θ	w (%)	
1	0.747 (±0.01)	0	37.5	Phenol (3)
		3.4	37.5	DMP (5)
		23.0	12.5	DCMP (10)
		25.6	12.5	DCDMP (10)
2	0.739 (±0.01)	0	37.5	Phenol (3)
		1.9	37.5	DMP (5)
		5	22.5	DCMP (10)
		10.9	20	DCDMP (10)
		11.4	12.5	
		24.8	12.5	
3	0.748 (±0.01)	0	37.5	DMP (5)
		2	37.5	DCDMP (10)
		5.1	22.5	
		11.3	20	
		11.8	12.5	
		25.7	12.5	

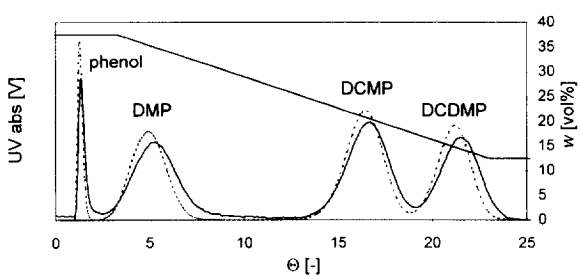

Fig. 4. Experimental (solid) and simulated (dashed) effluent concentration profiles and the applied gradient (1, see Table 4) for the separation of phenol, DMP, DCMP and DCDMP. ($\phi_v = 4$ ml/min, $\omega = 800$ rpm, $\varepsilon_s = 0.747$).

maximum deviation from the average value. It appears from Fig. 4 as if the model predicts peak widths that are smaller than the experimental peak widths, however, the simulated peak widths for DCMP and DCDMP are within the experimental error.

For 'normal' mode separations the peak width usually increases with increasing retention time. Due to the relationship between the overall volumetric mass transfer coefficient and the partition coefficient (Eq. (10)), peaks with higher partition coefficients (higher retention times) have a lower overall volumetric mass transfer coefficient and, therefore, show increased tailing [11]. However, Table 5 shows that the DMP, DCMP and DCDMP peaks have comparable peak widths. When the components are injected, they partition to a large extent to the stationary phase and hardly migrate through the column (they are 'fixed' in the first few channels of the column). If no gradient is applied, the peaks (especially DCMP and DCDMP) will have very high retention times and

Table 5
Experimental and predicted retention time and peak widths

Component	Experimental retention time (s)	Experimental peak width (s)	Predicted retention time (s)	Predicted peak width (s)
DMP	2060±2.8%	829±7.4%	1950	730
DCMP	6549±0.8%	778±9.3%	6380	774
DCDMP	8446±0.4%	748±5.1%	8310	704

peak widths. However, due to the gradient, the partition coefficients of the components decrease and the overall volumetric mass transfer coefficients increase. At a given composition of the mobile phase the partition coefficients come in the more suited range of migration through the column at a relatively low partition coefficient and high overall volumetric mass transfer coefficient. Due to the gradient, all the components migrate through the column at roughly the same partition coefficient and overall volumetric mass transfer coefficient, and therefore, have roughly the same peak width. It should be mentioned that this is only true for components that show the same partitioning behaviour (parallel lines in Fig. 2) as a function of the mobile phase gradient.

To determine the influence of $k_s a$ and $k_m a$ on the resolution, two simulations have been performed where $k_s a$ and $k_m a$ have been fixed at the values obtained for w is 12.5% (v/v) and for w is 37.5% (v/v), instead of interpolating between the three values for the different values of w. The deviation between the experimental and simulated peak widths changes only slightly (within the experimental error) compared to the simulated values obtained when using the interpolation method. Therefore, it is concluded that the resolution is not greatly effected by the $k_s a$ and $k_m a$ values for w in the range 12.5% (v/v) −37.5% (v/v). This might change when a system with $w<12.5\%$ is used.

Fig. 4 shows that the space (resolution) between peak 2 (DMP) and peak 3 (DCMP) is relatively large. Therefore, to decrease the total separation time and to show the usefulness of modelling gradient elution, a steeper gradient was applied. Furthermore, a second gradient 'step' was applied (before the elution of the DCDMP peak) to 'force' the last component of the column. In this way the peak width of the DCDMP peak should be minimised. The result is shown in Fig. 5. Again, the model prediction compares well to the experimental effluent concentration profile. The retention times of the experimental peaks are (again) smaller than the retention times of the simulated peaks, indicating a possible systematic error in the model parameters. The peak widths of the simulated peaks are also smaller than those of the experimental peaks. The total separation time compared to gradient 1 has been reduced by

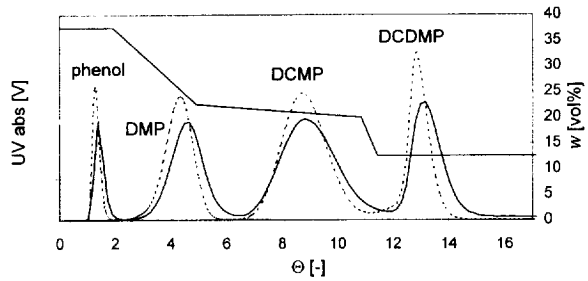

Fig. 5. Experimental (solid) and simulated (dashed) effluent concentration profiles and the applied gradient (2, see Table 4) for the separation of phenol, DMP, DCMP and DCDMP ($\phi_v = 4$ ml/min, $\omega = 800$ rpm, $\varepsilon_s = 0.739$).

roughly 30%. This is mainly because the resolution between the DMP peak and the DCMP peak has decreased, as predicted.

The exact position of the gradient 'steps' is very important for the shape of the peak as is shown in Fig. 6 for the elution of DMP and DCDMP with gradient 3. If the gradient 'steps' start too late, the peaks will show increased fronting. This is because part of the peak comes out with the 'normal' gradient, while the rest of the peak is 'forced' off the column during the gradient 'step'. The predicted effluent concentration profile compares well to the experimental effluent concentration profile. The DCDMP peak already shows fronting when gradient 2 is applied, however, this is not visible in due to the interference with the DCMP peak. A similar effect

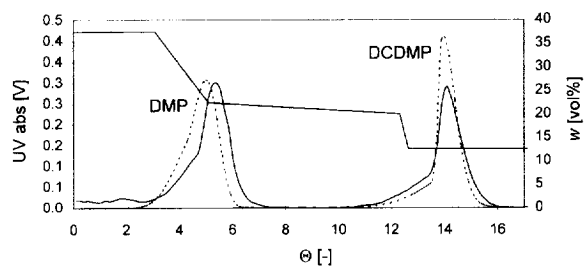

Fig. 6. Experimental (solid) and simulated (dashed) effluent concentration profiles and the applied gradient (3, see Table 4) for the separation of DMP and DCDMP ($\phi_v = 4$ ml/min, $\omega = 800$ rpm, $\varepsilon_s = 0.748$).

was found by Foucault and Nakanishi [7] who used the hexane–methanol–water two-phase system for the separation of a mixture of aromatic alcohols, an aldehyde and polyaromatic hydrocarbons. One of the aromatic alcohols, that eluted when the gradient is run, shows the same fronting peak behaviour as it is observed for DMP (Fig. 6).

5. Conclusions

A model is presented that describes effluent concentration profiles of gradient elution experiments in CPC. The model parameters that are needed to perform the model simulations are the flow-rate, stationary-phase hold-up and the column volume (separation conditions), and the partition coefficients of the components and a mass transfer relationship valid for the given separation conditions (including the rotational frequency). The partition coefficients and the mass transfer relationship should be known as a function of the composition of the mobile phase. The model predictions compare well to the experimental effluent concentration profiles. The partition coefficients of the components as a function of the gradient have the largest influence on the accuracy of the model predictions. The mass transfer relationship is less critical. This means that for optimisation of gradient elution separations, relatively simple shake flask experiments will be sufficient to obtain a good prediction of the experimental CPC effluent concentration profiles. For separation of components with a partition behaviour more complex than for the presented example, fine-tuning of the gradient by 'trial and error' would be difficult. In this case the model presented in this work can be a valuable tool.

6. Notation

a	specific interfacial area (m^2/m^3)
A_1, A_2	constants [Eq. (7)]
X	dimensionless mobile phase concentration (mol/m^3)
Y	dimensionless stationary phase concentration (mol/m^3)
$k_o a$	overall volumetric mass transfer coefficient (1/s)
$k_m a$	volumetric mass transfer coefficient in the mobile phase [1/s]
$k_s a$	volumetric mass transfer coefficient in the stationary phase (1/s)
K	partition coefficient
Pe	Péclet number
St	Stanton number
V	total column volume (m^3)
w	total volumetric water content of the two-phase system (vol%)
z	dimensionless column position

Greek

ε_s	stationary-phase hold-up
ϕ_v	flow-rate (m^3/s)
Θ	dimensionless time
τ	mobile phase residence time (s)

Indexes

i	component i
n	stage number

Acknowledgments

I. Meijer and J. de Graaf are thanked for measuring the partition coefficients and the overall volumetric mass transfer coefficients. Leon Janssen is thanked for performing the gradient elution experiments.

References

[1] M.J. van Buel, L.A.M. van der Wielen and K.Ch.A.M., Luyben, in A.P. Foucault (Editor), Centrifugal Partition Chromatography, (Chromatographic Science Series, Vol. 68), Marcel Dekker, New York, 1995, pp. 51–69.
[2] A.P. Foucault (Editor), Centrifugal Partition Chromatography (Chromatographic Science Series, Vol. 68), Marcel Dekker, New York, 1995.
[3] A. Berthod, Instr. Sci. Tech. 23 (1995) 75–89.
[4] A. Foucault, Anal. Chem. 64 (1991) 569A–579A.
[5] A. Marston, K. Hostettmann, J. Chromatogr. A 658 (1994) 315–341.
[6] W.D. Conway, ACS Symp. Ser. 593 (1995) 1–14.

[7] A. Foucault, K. Nakanishi, J. Liq. Chromatogr. 13 (1990) 3583–3602.
[8] W.D. Conway, Countercurrent Chromatography: Apparatus, Theory and Applications, VCH, New York, 1989.
[9] M. Vanhaelen, R. Vanhaelen-Fastré, J. Liq. Chromatogr. 11 (1988) 2969.
[10] A. Foucault, K. Nakanishi, J. Liq. Chromatogr. 12 (1989) 2587–2600.
[11] M.J. van Buel, L.A.M. van der Wielen, K.Ch.A.M. Luyben, J. AIChE 43 (1997) 693–702.
[12] G. Guiochon, S. Golshan Shirazi and A.M. Katti, Fundamentals of Preparative and Non-Linear Chromatography, Academic Press, Boston, MA, 1994, Chapters X and XI.